Multimodality Non-Rigid Image Registration for Planning, Targeting and Monitoring during CT-guided Percutaneous Liver Tumor Cryoablation

Haytham Elhawary, Ph.D., **Sota Oguro, M.D.**, **Kemal Tuncali, M.D.**, **Paul R. Morrison, MS**, **Servet Tatli, M.D.**, **Paul B. Shyn, M.D.**, **Stuart G. Silverman, M.D.**, and **Nobuhiko Hata, Ph.D.**
Department of Radiology, Brigham and Women's Hospital, Harvard Medical School, 75 Francis Street, Boston, MA, 02115, USA

Abstract

Rationale and Objectives—To develop non-rigid image registration between pre-procedure contrast enhanced MR images and intra-procedure unenhanced CT images, to enhance tumor visualization and localization during CT-guided liver tumor cryoablation procedures.

Materials and Methods—After IRB approval, a non-rigid registration (NRR) technique was evaluated with different pre-processing steps and algorithm parameters and compared to a standard rigid registration (RR) approach. The Dice Similarity Coefficient (DSC), Target Registration Error (TRE), 95% Hausdorff distance (HD) and total registration time (minutes) were compared using a two-sided Student's t-test. The entire registration method was then applied during five CT-guided liver cryoablation cases with the intra-procedural CT data transmitted directly from the CT scanner, with both accuracy and registration time evaluated.

Results—Selected optimal parameters for registration were section thickness of 5mm, cropping the field of view to 66% of its original size, manual segmentation of the liver, B-spline control grid of 5×5×5 and spatial sampling of 50,000 pixels. Mean 95% HD of 3.3mm (2.5x improvement compared to RR, p<0.05); mean DSC metric of 0.97 (13% increase); and mean TRE of 4.1mm (2.7x reduction) were measured. During the cryoablation procedure registration between the pre-procedure MR and the planning intra-procedure CT took a mean time of 10.6 minutes, the MR to targeting CT image took 4 minutes and MR to monitoring CT took 4.3 minutes. Mean registration accuracy was under 3.4mm.

Conclusion—Non-rigid registration allowed improved visualization of the tumor during interventional planning, targeting and evaluation of tumor coverage by the ice ball. Future work is focused on reducing segmentation time to make the method more clinically acceptable.

Keywords

non-rigid registration; B-Spline registration; liver tumor cryoablation; multimodal registration

Introduction

CT is used to guide percutaneous liver tumor cryoablation (1–7) and has proven particularly useful when the tumor is not visible with ultrasound (US) (4,5,8). CT can be used to plan the interventional approach, to facilitate the safe placement of the ablation applicators in the tumor and to monitor the ablation effects in the case of cryoablation (9).

Despite the benefits of CT, there can be challenges related to the lack of soft tissue contrast for liver tumors on unenhanced CT images, especially for small or poorly marginated tumors and where there are contra-indications to the use of intravenous contrast material (10). The tumor selected for ablation and the adjacent structures at risk for injury during the procedure may be invisible or poorly visible (11–13). Suboptimal visibility can lead to improper applicator placement resulting in inadequate ablation beyond the tumor margins or thermal injury to adjacent structures (14). In order to overcome this problem, the interventional radiologist often relies on a pre-procedure contrast-enhanced CT or MRI that depicts tumor margins and surrounding structures, including vascular anatomy. The radiologist then performs a mental correlation of the pre- and intra-procedure images to estimate tumor location, tumor boundaries and adjacent anatomical structures. This can be challenging as the liver position, shape and relation to extrahepatic structures may differ significantly between two exams.

Image registration, a technique that attempts to match and correlate two different image datasets, has been proposed to align pre-procedure and intra-procedure images (15,16). Most techniques for registering liver images rely on rigid registration approaches (17–19). The main drawback of the rigid registration technique is that it compensates only for rigid whole organ motion of the liver between datasets but not for liver deformation caused by patient breathing, motion or positional change, or deformation due to pressure from surrounding organs and the presence of any interventional instruments. Others have advanced these registration methods further by developing non-rigid registration techniques (20–24), which take into account deformation of the liver.

Non-rigid registration methods have yet to be successfully applied to the planning, targeting and monitoring phases of CT-guided liver cryoablation procedures. This can be ascribed to previous non-rigid registration methods being impractical to use during the time frame of a clinical procedure or requiring large amounts of computational capacity not readily available in most interventional environments (20,25). If these methods could be optimized in terms of computation and time requirements to provide registration in the order of a few minutes or less, they would become more practical for use in the clinical setting. The clinical acceptance of longer registration times is subject to how the normal procedure timing and workflow is affected.

The purpose of this work was to develop an accelerated approach to non-rigid image registration between pre-procedure contrast enhanced MR images and the intra-procedure unenhanced CT images acquired during CT-guided liver tumor cryoablation procedures. Firstly, to accelerate registration, we tested in a retrospective study several combinations of design parameters using a B-Spline based non-rigid registration method and chose those which provided the best compromise between accuracy, timing and robustness compared to a standard rigid registration approach. Secondly, we evaluated whether it was faster to directly register the pre-procedure MR image to each of the intra-procedure CT images acquired during the ablation, or whether resampling the pre-procedure MR image with the transformation matrices obtained form registering the intra-operative CT images between themselves would speed up the registration process. Once a suitable non-rigid registration method was developed, it was applied during five CT guided liver cryoablation procedures, with the intra-procedural CT data transmitted directly from the CT scanner to the workstation.

Materials and Methods

Patient Population

This study performed with IRB approval and in compliance with HIPAA guidelines analyzed MRI and CT images of fourteen patients who had undergone percutaneous CT-guided cryoablation of liver tumors at our institution from January to June of 2009. The patient medical records were reviewed to determine sex, age and diagnosis of each patient. Images from nine patients were retrieved from our departmental PACS archive for testing and optimization of the image registration technique. In the five remaining patients, images were transferred for analysis directly from the CT scanner during the liver cryoablation procedures, with the pre-procedure MR images previously retrieved from our PACS archive.

Patients had a mean age of 67 years (range 49 – 81) and mean liver tumor size of 35mm (range 15 – 65), with five tumors located in segment 7 of the liver, four tumors in segment 8, two in segment 5, two in segment 6 and one occupying both segments 2 and 3. For the nine patients whose images were retrieved from the PACS system, the tumors and tumor margins were visible using unenhanced CT images in two patients, tumors were faintly visible but with undefined margins in three patients and both tumors and margins were completely invisible in four patients. For the five patients whose images were transferred directly from the CT scanner, the tumor and margins were visible in one patient, faintly visible in two and invisible in the other two. All patients underwent CT-guided cryoablation of liver tumors, which required placement of an average of 5 applicators (range 4 – 7). The cryoablation procedure consisted of three phases. In the *planning* phase, an initial CT scan of the abdomen was used to select an optimal entry point and plan applicator placement. During the *targeting* phase, CT images were used to target the applicators at the planned locations. The *monitoring* phase employed CT images to demonstrate the effects of the cryoablation including the extent of the iceball.

Image Acquisition

The non-rigid registration method was used to register (i) pre-procedure contrast enhanced MR images to the intra-procedure unenhanced planning CT images, and (ii) intra-procedure CT images obtained at the targeting and monitoring phases of the intervention to the intra-procedure planning CT image. Pre-procedure MRI was obtained using a 1.5T SIGNA scanner (GE Healthcare, Waukesha, WI), using transverse fat-suppressed T1-weighted dynamic imaging with three dimensional (3D) fast-acquisition multiple-excitation spoiled gradient recalled echo sequence (TR/TE: 5.2–7.3/1.5–2.2ms; matrix size 512×512, flip angle 10°; section thickness 2.5mm; gap 0 mm; field of view 32–40 cm) with an 8 channel torso surface coil, after the intravenous administration of 20mL of gadolinium based contrast material (Magnevist, Berlex Laboratories, Wayne, NJ). Intra-procedure CT scans were performed on a 40 channel multi-detector row CT scanner (Sensation Open, Siemens Medical Solutions, Forchheim, Germany), with a matrix size of 512×512, 3mm section thickness, 0.6 mm collimation, 0.5 sec/rotation, 120kV and 168 to 398 mA.

Non-rigid and Rigid Registration Methods

We used a 3D volumetric non-rigid registration method which involved three steps: an approximate manual alignment between images, an affine transformation to model the global motion of the liver, followed by a B-Spline interpolation to describe local deformation (26). Both the affine and B-Spline registration techniques align the image volumes by maximizing mutual information, which is an image intensity based metric (27) implemented using the Mattes mutual information metric with multithreading. The affine method used 30 histogram bins to calculate mutual information and a one-plus-one evaluation optimization technique, where as the B-Spline method uses 100 histogram bins and a Flecther-Reeves-Polak-Ribiere (FRPR) gradient-line-search optimization.

The rigid registration technique also commenced with an approximate manual alignment between images followed by the calculation of a linear transformation with six degrees of freedom based on maximization of mutual information (27), using a one-plus-one evaluation optimization technique. Both registration methods were implemented using the ITK software library (www.itk.org).

The registration methods along with all pre-processing steps were implemented in 3D Slicer (www.slicer.org), an open source image visualization and processing software package developed previously at our center (28). The software was installed on a workstation with 4 Quad Core AMD Opteron 2.2GHz processors, 16GB of RAM with Ubuntu 9.2 operating system.

Registration Assessment Metrics

Once registration was complete, the livers were manually segmented from the resulting images. All image segmentations were performed by an interventional radiologist with 8 years experience (SO). Three methods were used to assess the accuracy of the registration. Firstly, the 95 percentile Hausdorff distance (95% HD), which measures the maximum perpendicular distance between points from the liver contours of the registered images (29). To calculate the 95% HD, the liver contours were extracted using a Canny Edge detector (30). Perfect alignment will produce a 95% Hausdorff distance of 0mm. A second metric was the Dice Similarity Coefficient (DSC) which measures volumetric overlap between the segmented livers from the registered images (31,32). The DSC can range from zero to one, where zero represents no alignment between registered livers and one represents perfect alignment. The third metric was the Target Registration Error (TRE), which is a measure of the Euclidian distance between well-defined anatomical features evident in both the registered image and the target image. To measure the TRE, three corresponding anatomical points were selected between the registered images. In 8 of the 9 cases the chosen anatomical structures of the liver were the main portal vein bifurcation, the umbilical portion and the first bifurcation of the right branch. However in one case these structures were not entirely visible on both images to make a reasonable measurement, and a point on the right, middle and left hepatic vein were chosen instead. Perfect alignment will yield a TRE of 0mm.

Optimization of Registration Between Pre-procedural MRI to Intra-procedural CT Images

In order to accelerate non-rigid registration between the pre-procedure contrast enhanced MRI and intra-procedure CT images, the latter obtained at the planning stage of the ablation procedure, a retrospective study from nine consecutive patients (mean age 63 years, range 49 – 72) who underwent ablation was performed. The objective of the study was to evaluate and understand how certain image characteristics, pre-processing steps and algorithmic parameters influence the accuracy, robustness and registration time of the non-rigid registration method. This was done in order to select the optimal set of parameters to accelerate the process as much as possible without compromising accuracy.

The optimization process of the non-rigid registration method was performed in two steps. The first step involved changing those parameters not related to the registration algorithm, such as section thickness, cropping of the image, field of view (FOV) and providing a segmented liver mask. Once the best set of parameters were chosen from this first step, the second step of the optimization process involved changing the resolution of the B-Spline control grid and the number of pixels used to calculate mutual information.

First Optimization Stage—Table 1 shows the different parameters that were studied in this first stage of the optimization process. Parameter set 1 acts as a reference set of parameters, and the other sets are defined by modifying a single parameter value from the reference set.

The first three parameter values consist of changing the section thickness of the images to 3mm, 5mm and 7.5mm. The next parameter set related to in-plane cropping, where the in-plane FOV varied from 100% of the acquired image, to 66% of the image and then to the smallest region surrounding the liver. The next parameter was manual segmentation of the liver to produce masked data. Registration was performed without masked data, with masked data obtained from manual segmentation of the liver, and with masked data obtained from manual segmentation of the liver from every other image section and with interpolation between the contours. Another parameter was cropping in the section thickness direction, with registration performed with over 75% of the liver volume included and then with between 50–75% of liver volume. This parameter was included to ensure that the registration method was robust even in the cases where only part of the liver has been imaged. For these tests, the B-spline control grid was set to 5×5×5, with the number of pixels used to calculate the mutual information metric 50,000 and 250,000 for affine and B-spline registration respectively. In total eight different parameter values were evaluated over nine patient datasets, giving a total of 72 registrations (Table 1). For each registration performed, the 95% HD and the total registration time were measured, and the best set of parameters was selected based on these values.

Second Optimization Stage—Table 2 shows the different algorithmic parameters that were evaluated for this second optimization stage. The resolution of the B-spline control grid was selected to be 3×3×3, 4×4×4 and 5×5×5. The number of total pixels randomly selected in the image to calculate the mutual information metric for both the affine and B-spline registration was varied in three categories: 2000, 20000 and 50000. In total six different parameter values were evaluated over nine patient datasets, giving a total of 54 registrations (Table 2). For each registration performed, the 95% HD and the total registration time were measured and the best set of parameters selected.

Comparison with Rigid Registration—Once the best set of parameters was chosen, the nine patient images were registered using both the rigid and optimized non-rigid registration methods. The 95% HD, the DSC and the TRE of the registered images were compared to quantify any improvement. A two-sided Student's t-test was used to measure any statistically significant differences of mean-values between the methods.

Registration of Intra-procedural CT Images

Registration between the pre-procedure MR images and the intra-procedure CT images was evaluated retrospectively on a subset of five patients using two different methods and their results compared. The first method involved directly registering the pre-procedure MR images to the planning CT image, then to the targeting CT image and finally to the monitoring CT image obtained during the CT-guided liver tumor ablation intervention. The second method involved an initial registration between the pre-procedure MR image to the planning CT image. Once the MR image was deformed and registered, the planning CT image was registered non-rigidly to the targeting CT image. The transformation matrix obtained from this CT to CT registration was then applied to the deformed MR image, previously registered to the planning CT image (Figure 1). A similar process was followed for registration to the monitoring CT image. Given the similarities between the multiple CT images obtained throughout the procedure in terms of patient positioning and voxel signal intensities, manual segmentation of the liver to provide masked data was not performed prior to registration. Knowledge of the algorithm and previous experience with the MR to CT registration suggested the following parameters: section thickness 3mm, no segmentation of the liver, no restrictions on liver volume, 5×5×5 B-spline spatial grid and 50,000 spatial samples to calculate mutual information. Once registration was completed, the livers were segmented from the images and the 95% HD, DSC and total registration time for each method was measured. Statistical differences between the methods were measured with a two sided Student t-test.

Registration during CT-guided Liver Tumor Ablation

To evaluate the entire non-rigid registration process, pre-procedure MR images were registered to intra-procedure CT images transmitted directly from the CT scanner to our computer workstation located adjacent to the interventional procedure room, during five CT-guided ablation procedures (patient mean age 61, range 49 – 70). The images were received at the workstation using a DICOM network protocol (DCMTK, dicom.offis.de, Germany). For the registration, the pre-procedure contrast enhanced MR images had been obtained from PACS and all pre-processing, such as cropping and manual segmentation of the images, was done several days before the intervention. The 95% HD and total registration time was quantified.

Results

Registration for Pre-procedural MR to Intra-procedural CT Images

The results of the evaluation of the registration parameters listed in Table 1 are presented in Figure 2. Accuracy based on the 95% HD ranged from 1.9 – 3.3mm (excluding set 6 which did not undergo segmentation or masking of the data). Furthermore, for many of the parameter sets, the standard deviation, which measures the variability of the individual registrations away from the average, was small indicating robustness of the method. The entire registration process required between 9.4 and 43.9 minutes. Parameter set 7, with a 95% HD of 2.8±0.4mm and a computation time of 19.3 minutes, was selected as the optimal protocol for our technique as it provided the best compromise between accuracy and registration time. This included a section thickness of 5mm, cropping the FOV to 66% of its original size and segmenting the liver on the images at every other section to create masked data. The results of the evaluation of registration parameters listed in Table 2, the second stage of the optimization process, are presented in Figure 3. Accuracy based on the 95% HD ranged from 3.6 – 5.6mm. The variation in registration parameters signified computation times ranging from 77 seconds for parameter set 1 to 48 seconds for parameter set 5, although it also produced a considerable increase in the registration error. Parameter set 1 was chosen over the others due to its increased accuracy and only marginally increased computation time, which is negligible when compared with the time required for pre-processing and segmentation. Figure 4 shows one case of non-rigid registration between pre-procedure contrast enhanced MR and intra-procedure planning CT images with these optimized parameters. Figure 5 shows the results obtained by comparing the optimized non-rigid registration technique and a rigid registration method on the nine patient images. Using non-rigid registration a 2.5 times improvement in the average 95% HD was obtained (non-rigid: 3.29mm, rigid: 7.96mm, $p<0.05$), 13% improvement in the average DSC metric (non-rigid: 0.97, rigid: 0.86, $p<0.05$) and a 2.7 fold reduction in the average TRE (non-rigid: 4.1mm, rigid: 11.04mm, $p<0.05$).

Registration of Intra-procedural CT Images

Table 3 shows the results of non-rigid registration of pre-procedure MR to the intra-procedure CT images using the two approaches. The first involved direct MR to CT registration, while the second had an indirect approach using the transformations obtained from CT to CT registrations. For the first method, the initial MR to planning CT registration took 19.2 minutes, with subsequent registrations performed in just over 10 minutes, as pre-processing and segmentation of the MR image did not need to be repeated. The indirect approach is statistically significantly faster, performing MR to targeting CT and MR to monitoring CT in less than 5 minutes once the initial pre-procedure MR image had been registered to the intra-procedure planning CT image. Accuracy was similar for both methods (no statistically significant differences), presenting average 95% HD of less than 4mm.

Registration during CT-guided Liver Tumor Ablation

Figure 6 shows the registration results for the non-rigid registration performed simultaneously during a clinical procedure and Figure 7 quantifies these results. The MR to planning CT registration yielded an average accuracy of 3.2±0.2mm (range 2.9–3.4mm), an average DSC of 0.96±0.01 (range 0.96 – 0.97) and registration time of 10.6±1.5 minutes (range 9–12 minutes). The MR to targeting CT registrations were completed in 4.9±1.2 minutes (range 4.1–7 minutes) and yielded an average 95% HD of 2.3±0.8mm (range 1.7–3.7mm) and DSC of 0.96±0.02 (range 0.94–0.98mm). The MR to monitoring CT registrations were completed in 4.3±0.7 minutes (range 4–5.7 minutes) and yielded an average 95% HD of 3.4±0.2mm (range 3.1–3.7mm) and DSC of 0.96±0.02 (range 0.93–0.98).

Discussion

We have presented the evaluation of a multi-modality non-rigid registration method which can enhance visualization of tumor margins and location during the planning, targeting and monitoring phases of CT-guided cryoablation procedures. We have shown that the method, when used with an optimized set of parameters, is considerably more accurate than rigid registration. In addition we have demonstrated that it is more efficient to perform an initial registration between pre-procedure MRI and intra-procedure planning CT, and then to register the deformed MR image to the rest of intra-procedure CT images using transformations obtained from CT to CT registration.

Non-rigid registration is desirable to compensate for liver deformation caused by patient positioning, respiratory motion and interventional manipulation (24). Non-rigid registration techniques are characterized by their capacity to estimate both global and local deformations of tissue, and as such, are often based on algorithms which are computationally demanding and impractical for real-time use during clinical procedures. Several non-rigid registration techniques have been reported (15,16,25,26,33–35), with only some applied to the liver (20–24,36). Niculescu et al. (21) registered pre-procedure and post-ablation CT images by using a surface-based, non-rigid registration method with a finite element model to simulate volumetric deformation. However, in (21), the method's accuracy was not assessed quantitatively. Archip et al. (20) compared several non-rigid registration techniques to match pre-procedure contrast enhanced MRI of the liver to intra-procedure CT images, including a finite element based method previously developed for neurosurgery (25). Substantial processing of the pre-procedure images was done prior to the intervention, and the finite element method had to be run on a computer cluster at a high performance computational infrastructure at a separate facility in order to run in a clinically feasible time frame (25).

Three important factors should be considered for the adequate translation of a registration technique into the clinical setting. The registration method should be *(i)* accurate for the clinical application, *(ii)* fast enough to be performed within the time frame of a clinical intervention (within a few minutes) and *(iii)* robust so that it almost never fails. The non-rigid registration method evaluated in this paper was optimized in order to choose those parameters which would accelerate the registration without compromising accuracy. More importantly, however, this process identified which components of the registration need to be improved to significantly reduce registration time. Considering this criteria, the optimal parameters were 5mm image section thickness, cropping at 66% of the FOV, masked liver data with segmenting performed every other slice, B-spline control grid 5×5×5 and 50,000 spatial samples. Considering *accuracy*, the reported 3.3mm (95% HD) average accuracy of the non-rigid registration method was considerably better than the 7.96mm measured using rigid registration (Figure 5). The 3.3mm average error using non-rigid registration should be satisfactory for liver tumor ablation, as the average tumor size was 35mm, much larger than the error. Although the optimization process revealed settings that provided increased accuracy, the chosen settings seemed to

present the best compromise between registration time and accuracy. This result is similar to the biomechanical model reported by Archip et al (20) which presented an average accuracy of 1.6mm and to the 2.2mm average accuracy reported by Lange et al (36) who used a method based on vessel location within the liver. Our results were considerably better than the method by Rohlfing et al (24) who reported an average accuracy of 10mm. The accuracy decreased considerably when manual segmentation of the liver was not performed, and therefore segmentation is essential to the method. Considering time, segmentation is by far the most time consuming step in the process taking between 12–20 minutes. One way of reducing segmentation time was to increase section thickness, such that there were fewer sections per volume. However at 7.5mm section thickness, the registration error increased while image resolution decreased. Another way to speed up segmentation was to segment the liver only every other slice, which provided a good mask while reducing segmentation time to 12 minutes. Considering robustness, for cropping both in-plane (trans-axial) and in the slice direction (z-axis), the algorithm performed extremely well, hence incomplete image acquisitions of the liver during the cryoablation procedure should have little effect. This can be especially relevant as often the intra-procedure CT images only include a portion of the liver organ in order to reduce radiation exposure. For many of the parameter sets, the standard deviation, which measures the variability of the individual registrations, was small, indicating another indirect measure of the method's robustness. The standard deviation did increase considerably however when lower sized B-Spline control grids and fewer spatial samples were selected to calculate mutual information, which discarded their recommendation for the clinic.

In contrast with MR to CT registration, CT to CT is less demanding on the non-rigid registration method as patient position is relatively stable between scans, and voxel signal intensities are comparable due to the images being from the same imaging modality. Hence registration time was comparatively lower, and MR to CT registration using transformations from CT to CT can be performed in an average of less than 5 minutes. Average accuracy was 3.3mm which was achieved without the need for manual segmentation of the liver. In addition, the method was robust even with the presence of applicator artifacts.

When considering the suitability of the non-rigid registration method for prospective clinical application during CT-guided ablation, we expect that the initial MR to CT registration, which takes 10.6 minutes when pre-processing and segmentation of the MR images are done before the procedure, could potentially be performed while the patient is undergoing preparation, sterilization of the surgical field and anesthesia. Subsequent registrations can be performed much faster (4–5 minutes). During the targeting phase, images are taken very frequently to guide the applicator probes into the planned tumor location. Since this process requires a constant iteration between applicator placement and imaging, the registration time would considerably delay the procedure and hinder the workflow. Instead the MR to targeting CT registration, which takes 4–5 minutes, must be performed once all the applicators have been located, and used to confirm that the location of the probes is such that the interventional radiologist can be confident of tumor coverage. Finally, during the monitoring phase, images are taken at certain intervals to monitor the formation of the ice ball and ensure coverage. Registration could thus be performed while the ice ball is at its largest size so as to ensure complete coverage of the tumor. In general though, the authors of this study consider that a few minutes for registration time is generally accepted, with longer times being subject to how they affect the normal procedure timing and workflow. Hence, although these registration times are close to being short enough for use during clinical applications, we believe they are still too long to be clinically feasible. It is difficult to compare our registration time with similar non-rigid registration methods reported in literature, since most studies only report accuracy of their methods. Some studies report computation time for their registration process, but total registration time, which includes computation and preprocessing time, is rarely reported. In addition, when comparing total computation time, it is important to consider the hardware used,

as it will greatly affect the computation. Lange et al (23,36) report a total run-time for computation of approximately one hour on a single processor machine, but no information on total registration time is given. Yen Wei et al (22) reports a computation time of 15 minutes without any information about hardware. Manual segmentation, which is a crucial step to achieve accuracy of the registration method, is the most time-consuming step of the method and any improvements in this pre-processing step would considerably reduce the total registration time. Hence future work will be focused on investigating fast and accurate semi-automatic and automatic segmentation methods, many of which have been reported in literature (37). In addition, these segmentation techniques would relieve the need for an experienced radiologist to manually segment the liver. It is also possible to reduce registration time by evaluating strategies which can shorten the computation time, both for MR to CT and CT to CT registration. This would include using computationally efficient mutual information estimation as described in recent work by Gholipour et al. (38) or by experimenting with the registration optimization method, multi-resolution strategies and convergence criteria (39, 40). However, since computation time is currently only 5–7% of total registration time, the impact of these strategies is somewhat limited.

A limitation of our study is the small number of subjects used. With larger series and prospective use, the method must demonstrate its robustness and accuracy with the expected anatomical variability expected of larger patient populations. Another limitation is the fact that a single radiologist performed the manual segmentation of all the images during the registration method, and hence inter-observer variability was not assessed in this study.

In conclusion, we optimized and evaluated a non-rigid registration method for use during CT-guided liver cryoablation. Further work is required to reduce segmentation time, which in turn will increase acceptance of the method during CT-guided ablation procedures. The method did however prove to be robust and accurate, and was capable of registering both MRI to CT and CT to CT images, which is a considerable improvement with respect to the current state of the art in the field. This is important as it may potentially improve tumor visualization during the planning, targeting and monitoring phases of CT-guided percutaneous liver ablation.

Acknowledgments

References

1. Antoch G, Kuehl H, Vogt FM, Debatin JF, Stattaus J. Value of CT volume imaging for optimal placement of radiofrequency ablation probes in liver lesions. J Vasc Interv Radiol Nov;2002 13(11): 1155–1161. [PubMed: 12427816]

2. Jakobs TF, Hoffmann RT, Schrader A, et al. CT-guided radiofrequency ablation in patients with hepatic metastases from breast cancer. Cardiovasc Intervent Radiol Jan;2009 32(1):38–46. [PubMed: 18575933]

3. Kuehl H, Stattaus J, Forsting M, Antoch G. Transhepatic CT-guided radiofrequency ablation of adrenal metastases from hepatocellular carcinoma. Cardiovasc Intervent Radiol Nov–Dec;2008 31(6):1210–1214. [PubMed: 18584241]

4. Ohmoto K, Mimura N, Iguchi Y, et al. CT-guided percutaneous ethanol injection therapy for ultrasonically invisible hepatocellular carcinoma. Hepatogastroenterology Mar–Apr;2002 49(44): 297–299. [PubMed: 11995437]

5. Sato M, Watanabe Y, Tokui K, Kawachi K, Sugata S, Ikezoe J. CT-guided treatment of ultrasonically invisible hepatocellular carcinoma. Am J Gastroenterol Aug;2000 95(8):2102–2106. [PubMed: 10950066]

6. Shankar S, Bhargava P, Habib F, Desai M, Tyagi G, Whalen G. Transpulmonary CT-guided radiofrequency ablation of liver metastasis. Cardiovasc Intervent Radiol Jul–Aug;2005 28(4):481–484. [PubMed: 16001134]

7. Shankar S, Tuncali K, vanSonnenberg E, Seifter JL, Silverman SG. Myoglobinemia after CT-guided radiofrequency ablation of a hepatic metastasis. AJR Am J Roentgenol Feb;2002 178(2):359–361. [PubMed: 11804892]

8. Park BJ, Byun JH, Jin YH, et al. CT-guided radiofrequency ablation for hepatocellular carcinomas that were undetectable at US: therapeutic effectiveness and safety. J Vasc Interv Radiol Apr;2009 20 (4):490–499. [PubMed: 19328427]

9. Silverman SG, Tuncali K, Morrison PR. MR Imaging-guided Percutaneous Tumor Ablation. Academic Radiology 2005;12(9):1100–1109. [PubMed: 16099689]

10. Clasen S, Pereira PL. Magnetic resonance guidance for radiofrequency ablation of liver tumors. J Magn Reson Imaging Feb;2008 27(2):421–433. [PubMed: 18219677]

11. Lu DS, Raman SS, Vodopich DJ, Wang M, Sayre J, Lassman C. Effect of vessel size on creation of hepatic radiofrequency lesions in pigs: assessment of the "heat sink" effect. AJR Am J Roentgenol Jan;2002 178(1):47–51. [PubMed: 11756085]

12. Goldberg SN, Hahn PF, Tanabe KK, et al. Percutaneous radiofrequency tissue ablation: does perfusion-mediated tissue cooling limit coagulation necrosis? J Vasc Interv Radiol Jan–Feb;1998 9 (1 Pt 1):101–111. [PubMed: 9468403]

13. Mahnken AH, Buecker A, Spuentrup E, et al. MR-guided radiofrequency ablation of hepatic malignancies at 1.5 T: initial results. J Magn Reson Imaging Mar;2004 19(3):342–348. [PubMed: 14994303]

14. Livraghi T, Solbiati L, Meloni MF, Gazelle GS, Halpern EF, Goldberg SN. Treatment of Focal Liver Tumors with Percutaneous Radio-frequency Ablation: Complications Encountered in a Multicenter Study. Radiology February 1;2003 226(2):441–451. [PubMed: 12563138]

15. Crum WR, Hartkens T, Hill DLG. Non-rigid image registration: theory and practice. Br J Radiol December 1;2004 77(suppl_2):S140–153. [PubMed: 15677356]

16. Hill DLG, Batchelor PG, Holden M, Hawkes DJ. Medical image registration. Physics in Medicine and Biology 2001;46(3):R1–R45. [PubMed: 11277237]

17. Carrillo A, Duerk JL, Lewin JS, Wilson DL. Semiautomatic 3-D image registration as applied to interventional MRI liver cancer treatment. Medical Imaging, IEEE Transactions on 2000;19(3):175–185.

18. Wilson DL, Carrillo A, Zheng L, Genc A, Duerk JL, Lewin JS. Evaluation of 3D image registration as applied to MR-guided thermal treatment of liver cancer. Journal of Magnetic Resonance Imaging 1998;8(1):77–84. [PubMed: 9500264]

19. Penney GP, Blackall JM, Hamady MS, Sabharwal T, Adam A, Hawkes DJ. Registration of freehand 3D ultrasound and magnetic resonance liver images. Medical Image Analysis 2004;8(1):81–91. [PubMed: 14644148]

20. Archip N, Tatli S, Morrison P, Jolesz F, Warfield S, Silverman S. Non-rigid Registration of Pre-procedural MR Images with Intra-procedural Unenhanced CT Images for Improved Targeting of Tumors During Liver Radiofrequency Ablations. Medical Image Computing and Computer-Assisted Intervention – MICCAI 2007 2007:969–977.

21. Niculescu, G.; Forand, DJ.; Nosher, J. Non-rigid Registration of the Liver in Consecutive CT Studies for Assessment of Tumor Response to Radiofrequency Ablation. Paper presented at: Engineering in Medicine and Biology Society, 2007. EMBS 2007. 29th Annual International Conference of the IEEE; 2007.

22. Yen-Wei, C.; Katsumi, T.; Rui, X.; Shigehiro, M.; Yoshimasa, K. Semiautomatic non-rigid 3-D image registration for MR-Guided Liver Cancer Surgery. Paper presented at: Image Processing, 2008. ICIP 2008. 15th IEEE International Conference; 2008.

23. Lange T, Wenckebach TH, Lamecker H, et al. Registration of different phases of contrast-enhanced CT/MRI data for computer-assisted liver surgery planning: Evaluation of state-of-the-art methods. The International Journal of Medical Robotics and Computer Assisted Surgery 2005;1(3):6–20.

24. Rohlfing T, Maurer CR Jr, O'Dell WG, Zhong J. Modeling liver motion and deformation during the respiratory cycle using intensity-based nonrigid registration of gated MR images. Med Phys Mar; 2004 31(3):427–432. [PubMed: 15070239]

25. Archip N, Clatz O, Whalen S, et al. Non-rigid alignment of pre-operative MRI, fMRI, and DT-MRI with intra-operative MRI for enhanced visualization and navigation in image-guided neurosurgery. Neuroimage Apr 1;2007 35(2):609–624. [PubMed: 17289403]

26. Rueckert D, Sonoda LI, Hayes C, Hill DLG, Leach MO, Hawkes DJ. Nonrigid registration using free-form deformations: application to breast MR images. Medical Imaging, IEEE Transactions on 1999;18(8):712–721.

27. Wells W, Viola P, Atsumi H, Nakajima S, Kikinis R. Multi-modal volume registration by maximization of mutual information. Med Image Anal 1996;03

28. Gering DT, Nabavi A, Kikinis R, et al. An integrated visualization system for surgical planning and guidance using image fusion and an open MR. J Magn Reson Imag 2001;13(6):967–975.

29. Hausdorff, F. Set Theory. 2. Chelsea Publication Company; 1962.

30. Canny J. A computational approach to edge detection. IEEE Trans Pattern Anal Mach Intell 1986;8 (6):679–698.

31. Bharatha A, Hirose M, Hata N, et al. Evaluation of three-dimensional finite element-based deformable registration of pre- and intraoperative prostate imaging. Med Phys Dec;2001 28(12):2551–2560. [PubMed: 11797960]

32. Zou KH, Warfield SK, Bharatha A, et al. Statistical validation of image segmentation quality based on a spatial overlap index1: scientific reports. Academic Radiology 2004;11(2):178–189. [PubMed: 14974593]

33. Morten, B-N.; Claus, G. Fast Fluid Registration of Medical Images. Proceedings of the 4th International Conference on Visualization in Biomedical Computing; Springer-Verlag; 1996.

34. Studholme C, Hill DLG, Hawkes DJ. An overlap invariant entropy measure of 3D medical image alignment. Pattern Recognition 1999;32(1):71–86.

35. Thirion JP. Image matching as a diffusion process: an analogy with Maxwell's demons. Med Image Anal Sep;1998 2(3):243–260. [PubMed: 9873902]

36. Lange T, Eulenstein S, Hunerbein M, Schlag PM. Vessel-based non-rigid registration of MR/CT and 3D ultrasound for navigation in liver surgery. Comput Aided Surg 2003;8(5):228–240. [PubMed: 15529952]

37. Heimann T, van Ginneken B, Styner MA, et al. Comparison and evaluation of methods for liver segmentation from CT datasets. IEEE Trans Med Imaging Aug;2009 28(8):1251–1265. [PubMed: 19211338]

38. Gholipour, A.; Kehtarnavaz, ND. Computationally efficient mutual information estimation for non-rigid image registration. Paper presented at: IEEE International Conference of Image Processing; 2008.

39. Klein S, Staring M, Pluim JPW. Evaluation of Optimization Methods for Nonrigid Medical Image Registration Using Mutual Information and B-Splines. Image Processing, IEEE Transactions on 2007;16(12):2879–2890.

40. Maes F, Vandermeulen D, Suetens P. Comparative evaluation of multiresolution optimization strategies for multimodality image registration by maximization of mutual information. Med Image Anal Dec;1999 3(4):373–386. [PubMed: 10709702]
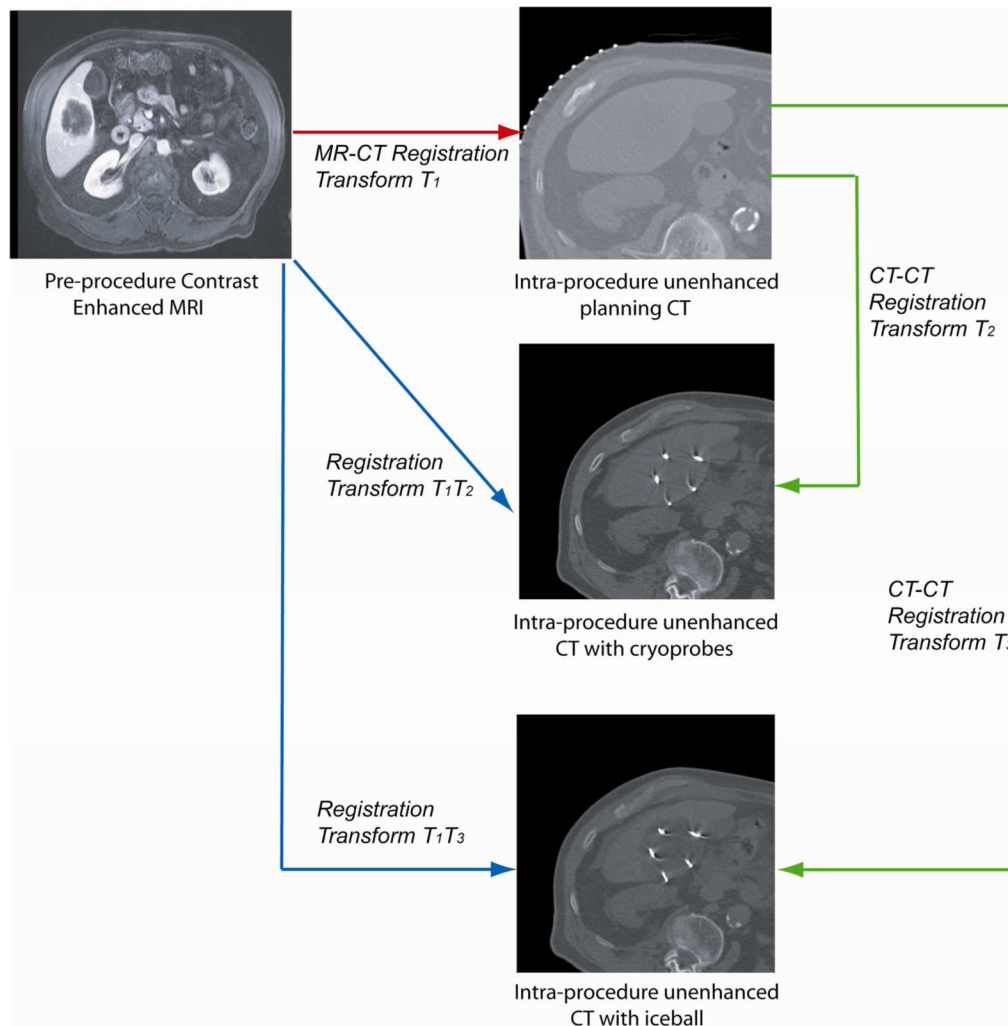
Figure 1.
Registration between the pre-procedure MRI and the intra-procedure planning CT image results in a transformation matrix T1, which was used to deform the pre-procedure MRI on to the intra-procedure planning CT image. To register the pre-procedure MRI to both the intra-procedure targeting and monitoring CT images, we registered the planning CT image to the targeting CT image and the resulting transformation matrix T2 was combined with T1, to deform the pre-procedure MR image onto the targeting CT image. The same process can be applied to the monitoring CT image.
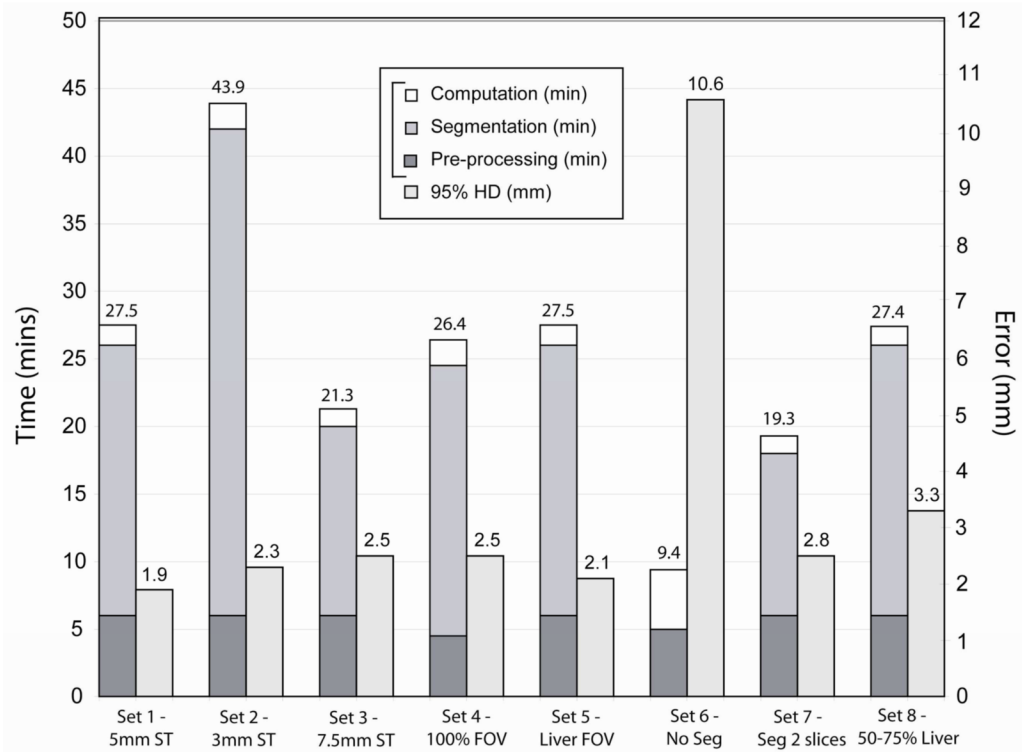
Figure 2.
The graph indicates for each set of parameters (Table 1) the average time taken to perform the entire registration as well as the average 95% Hausdorff distance as an indicator of accuracy.
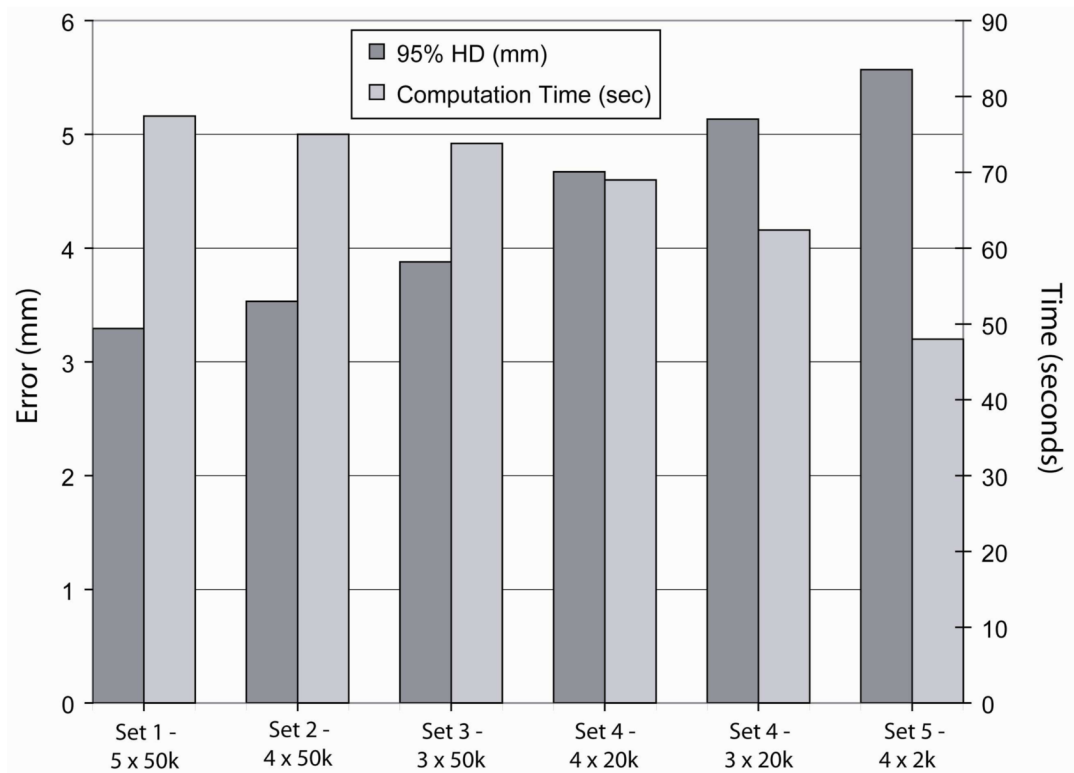
Figure 3.
The graph indicates for each set of design parameters related with the registration algorithm (Table 2), the average computation time taken to perform the non-rigid registration as well as the average 95% Hausdorff distance as an indicator of accuracy.
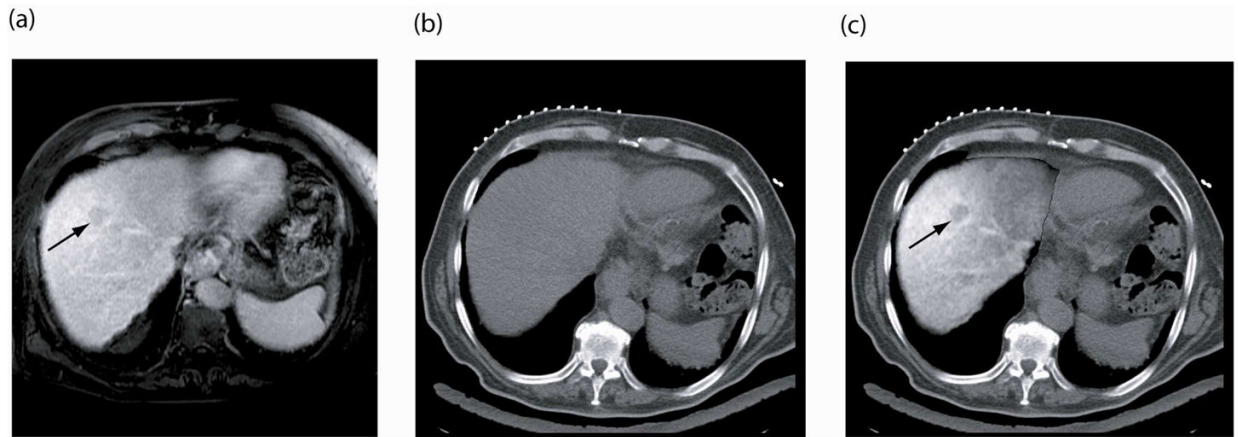
Figure 4.
(a) Pre-procedure, contrast-enhanced MRI shows 3cm liver tumor (arrow), (b) intra-procedure unenhanced CT image does not show the tumor, and (c) registration and fusion of the two images shows the MRI depicted tumor overlaid on the intra-procedural CT image.
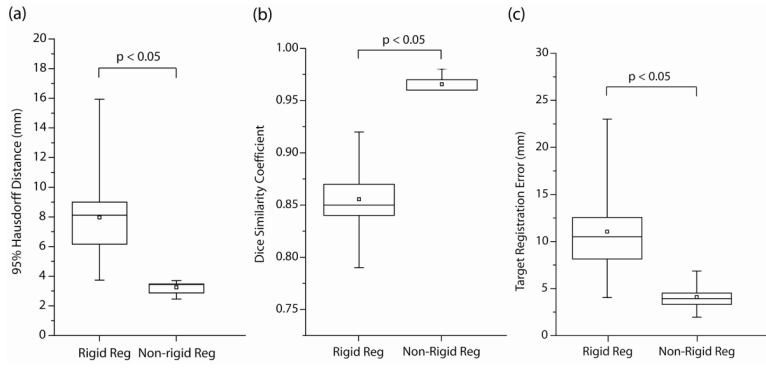
Figure 5.
Validation results for both rigid and non-rigid registration performed on nine patient images. The 95% Hausdorff Distance (HD), the Dice Similarity Coefficient (DSC) and the Target Registration Error (TRE) were measured in each case, showing a considerable improvement in all three metrics when using non-rigid registration compared to a rigid algorithm.
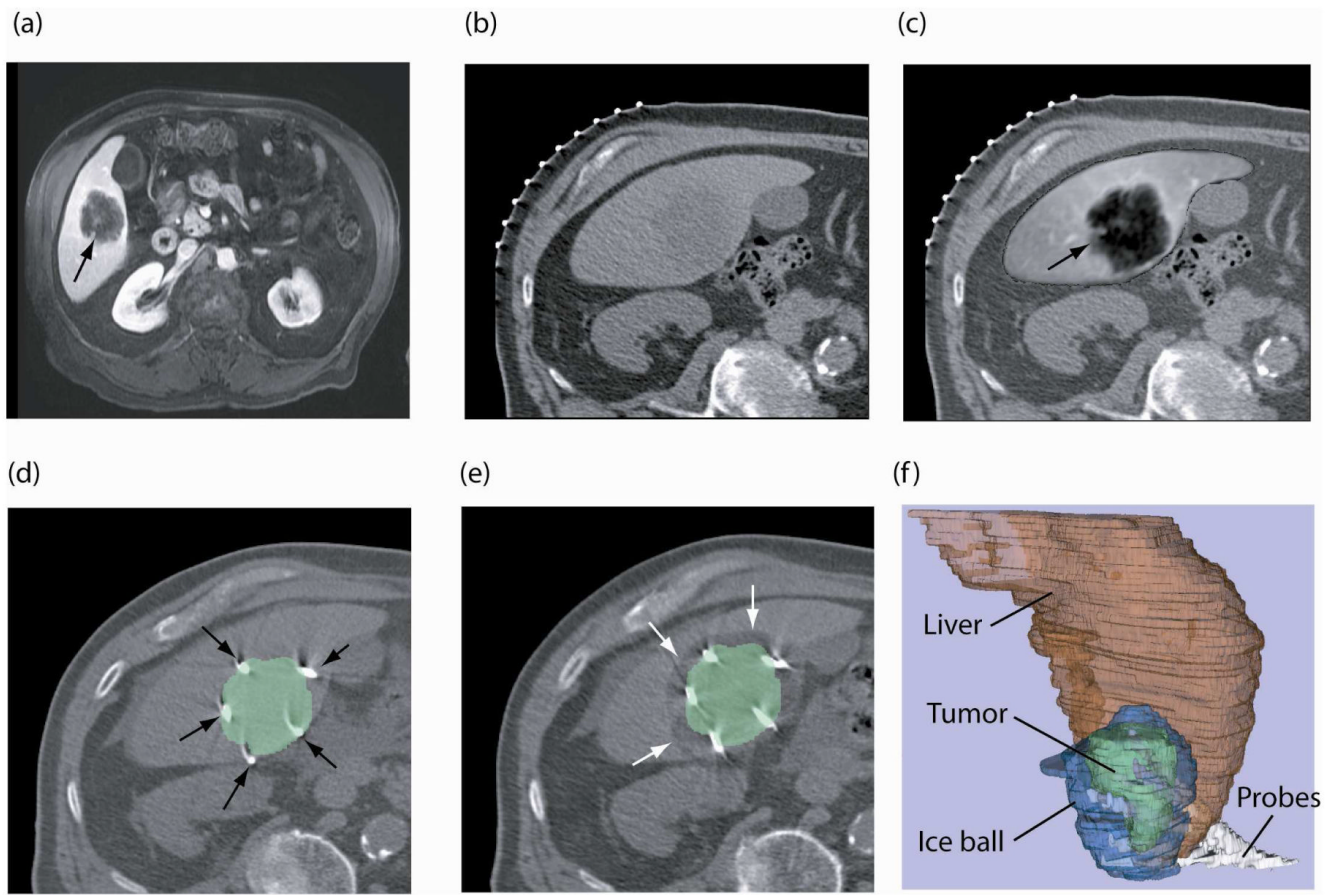
Figure 6.
(a) Pre-procedure, contrast-enhanced axial MR image obtained with patient in supine position shows tumor (arrow) as hypointense region, (b) intra-procedure CT image for interventional planning obtained with the patient in a left posterior oblique position, (c) registered and fused image shows liver tumor (arrow) from registered MR image overlaid on planning CT image, (d) targeting CT image shows cryoablation applicators (arrows) in position, overlaid with segmented tumor from the registered MR image, (e) CT image shows the iceball as hypointense area around the tumor (white arrows) overlaid with segmented tumor from registered MR image, and (f) 3D representation of liver, tumor, iceball and cryoablation applicators to evaluate tumor coverage and margins.
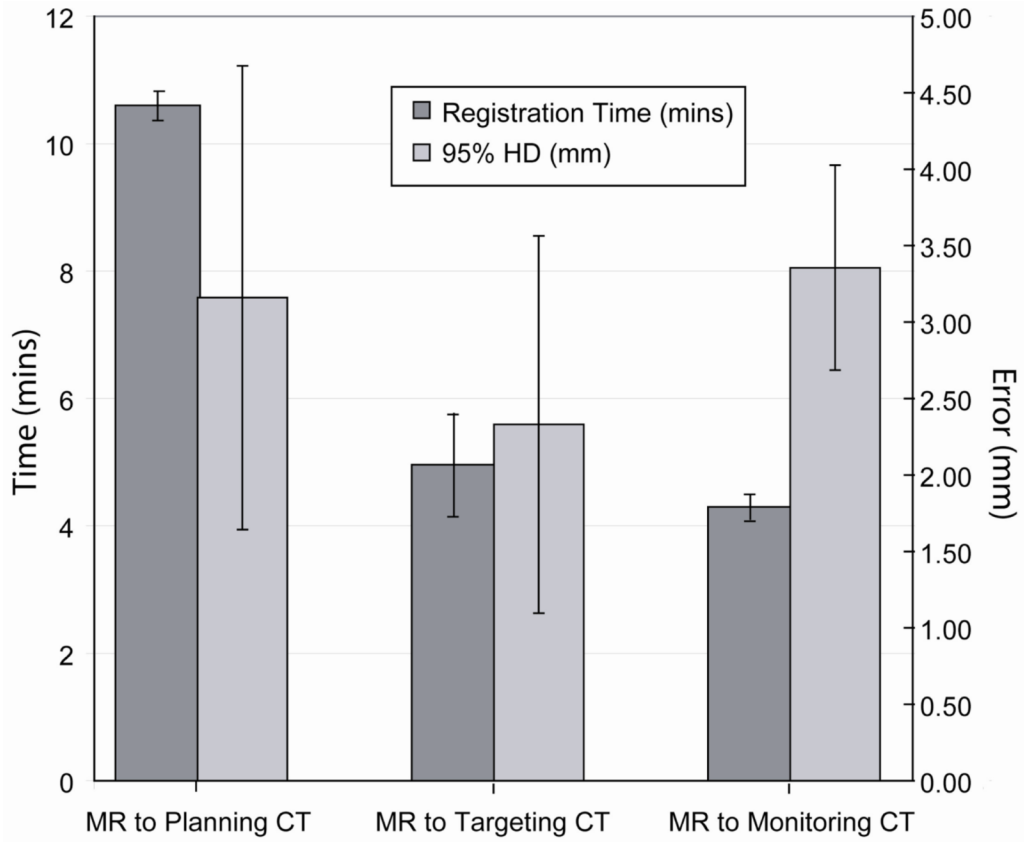
Figure 7.
The average time for registration and 95% Hausdorff Distance measured for non-rigid registration performed during CT-guided percutaneous liver tumor ablation. Registration was performed for pre-procedure MR and intra-procedure planning CT images; for MR and targeting CT images, and for MR and monitoring CT images acquired during the intervention. A standard deviation is also expressed around the average for each measured metric.

Table 1

Experiments performed to evaluate the effect of different parameters and preprocessing steps on the accuracy and time of the non-rigid registration method between pre-procedure contrast enhanced MRI and intra-procedure unenhanced CT images. Parameter set 1 acts as a reference set of parameters, and the other sets are defined by modifying a single parameter value from the reference set.

Parameter Set	Section Thickness (mm)	Field of View Size	Segmentation	Liver Volume
1 (Ref)	5	66%	Yes	>75%
2	3	66%	Yes	>75%
3	7.5	66%	Yes	>75%
4	5	100%	Yes	>75%
5	5	Liver	Yes	>75%
6	5	66%	No	>75%
7	5	66%	Every 2 slices	>75%
8	5	66%	Yes	50 – 75%

Table 2

Experiments performed to evaluate the effect of different algorithmic parameters on the accuracy and time of the non-rigid registration method between pre-procedure contrast enhanced MRI and intra-procedure unenhanced CT images.

Parameter Set	Number of Control Points per direction	Sampling Pixels
1 (Ref)	5	50,000
2	4	50,000
3	3	50,000
4	4	20,000
5	3	20,000
6	4	2,000

Table 3

Average 95% Hausdorff Distance (HD), Dice Similarity Coefficient (DSC) and total registration time measured for the two liver registration methods for five patient datasets. The first method was a direct registration of pre-procedure MR to the intra-procedure CT images, while the second method used the transformation obtained from CT to CT registration to deform and register the MR image.

Registered Images	Method 1			Method 2		
	95% HD (mm)	DSC	Time (min)	95% HD (mm)	DSC	Time (min)
MR – Planning CT	3.29	0.97	19.2	3.29	0.97	19.2
MR – Targeting CT	3.9	0.94	10.2	3.5	0.96	4.6
MR – Monitoring CT	3.9	0.93	10.4	4	0.96	4.3